PB85-227528

Dosimetry for In-vitro Chick Brain Calcium-Ion Efflux Experiments by Numerical Methods Based on Zonal Harmonic Expansions

Miami Univ., Coral Gables, FL

Prepared for

Health Effects Research Lab.
Research Triangle Park, NC

Jun 85

U.S. Department of Commerce
National Technical Information Service
NTIS

TECHNICAL REPORT DATA
(Please read Instructions on the reverse before completing)

1. REPORT NO. EPA/600/1-85/016	2.
3. RECIPIENT'S ACCESSION NO. PB85 227287/AS	
4. TITLE AND SUBTITLE Dosimetry for In Vitro Chick Brain Calcium-Ion Efflux Experiments by Numerical Methods Based on Zonal Harmonic Expansions	5. REPORT DATE June 1985
	6. PERFORMING ORGANIZATION CODE
7. AUTHOR(S) Guillermo Gonzalez and James Nearing	8. PERFORMING ORGANIZATION REPORT NO.
9. PERFORMING ORGANIZATION NAME AND ADDRESS Departments of Engineering and Physics University of Miami Coral Gables, Florida 33124	10. PROGRAM ELEMENT NO. CCGF1A
	11. CONTRACT/GRANT NO. 68-02-4092
12. SPONSORING AGENCY NAME AND ADDRESS Health Effects Research Laboratory Office of Research and Development US Environmental Protection Agency Research Triangle Park, NC 27711	13. TYPE OF REPORT AND PERIOD COVERED
	14. SPONSORING AGENCY CODE EPA-600/11
15. SUPPLEMENTARY NOTES	

16. ABSTRACT

This report discusses the calculation of the electric field and power density distribution in chick brain tissue inside a test tube, using an off-center spherical model. It is shown that the off-center spherical model overcomes many of the limitations of the concentric spherical model, and permits a more realistic modeling of the brain tissue as it sits in the bottom of the test tube surrounded by buffer solution. The effect of the unequal amount of buffer solution above the upper and below the lower surface of the brain is evaluated.

The field distribution is obtained in terms of a rapidly converging series of zonal harmonics. A method that permits the expansion of spherical harmonics about an off-center origin in terms of spherical harmonics at the origin is developed to calculate in closed form the electric field distribution.

Humerical results are presented for the absorbed power density distribution at carrier frequencies of 50 MHz, 100 MHz, and 147 MHz. It is shown that the absorbed power density is higher toward the bottom of the brain surface. Scaling relations are developed by keeping the electric field intensity in the brain tissue the same at two different frequencies. Scaling relations inside, as well as outside, the brain surface are given. The scaling relation distribution is calculated as a function of position, and compared to the scaling relations obtained in the concentric spherical model.

17. KEY WORDS AND DOCUMENT ANALYSIS

a. DESCRIPTORS	b. IDENTIFIERS/OPEN ENDED TERMS	c. COSATI Field/Group

18. DISTRIBUTION STATEMENT RELEASE TO PUBLIC	19. SECURITY CLASS *(This Report)* UNCLASSIFIED	21. NO. OF PAGES 39
	20. SECURITY CLASS *(This page)* UNCLASSIFIED	22. PRICE

EPA Form 2220-1 (Rev. 4-77) PREVIOUS EDITION IS OBSOLETE

EPA/600/1-85/016
June 1985
PB85-227528

DOSIMETRY FOR IN-VITRO CHICK BRAIN CALCIUM-ION EFFLUX EXPERIMENTS BY NUMERICAL METHODS BASED ON ZONAL HARMONIC EXPANSIONS

by

Guillermo Gonzalez
Department of Electrical and Computer Engineering
University of Miami
Coral Gables, Florida 33124

and

James C. Nearing
Department of Physics
University of Miami
Coral Gables, Florida 33124

68-02-4092

Project Officer

Ronald J. Spiegel
Experimental Biology Division
U.S. Environmental Protection Agency
Research Triangle Park, North Carolina 27711

U.S. Environmental Protection Agency
Health Effects Research Laboratories
Research Triangle Park, North Carolina 27711

REPRODUCED BY
NATIONAL TECHNICAL
INFORMATION SERVICE
U.S. DEPARTMENT OF COMMERCE
SPRINGFIELD, VA. 22161

DISCLAIMER

The information in this document has been funded wholly or in part by the United States Environmental Protection Agency under contract 68-02-4092. It has been subject to the Agency's peer and administrative review, and it has been approved for publication as an EPA document. Approval does not signify that the contents necessarily reflect the views and policies of the U.S. Environmental Protection Agency, nor does mention of trade names or commercial products constitute endorsement or recommendation for use.

ABSTRACT

This report discusses the calculation of the electric field and power density distribution in chick brain tissue inside a test tube, using an off-center spherical model. It is shown that the off-center spherical model overcomes many of the limitations of the concentric spherical model, and permits a more realistic modeling of the brain tissue as it sits in the bottom of the test tube surrounded by buffer solution. The effect of the unequal amount of buffer solution above the upper and below the lower surface of the brain is evaluated.

The field distribution is obtained in terms of a rapidly converging series of zonal harmonics. A method that permits the expansion of spherical harmonics about an off-center origin in terms of spherical harmonics at the origin is developed to calculate in closed form the electric field distribution.

Numerical results are presented for the absorbed power density distribution at carrier frequencies of 50 MHz, 100 MHz and 147 MHz. It is shown that the absorbed power density is higher toward the bottom of the brain surface.

Scaling relations are developed by keeping the electric field intensity in the brain tissue the same at two different frequencies. Scaling relations inside, as well as outside, the brain surface are given. The scaling relation distribution is calculated as a function of position, and compared to the scaling relations obtained in the concentric spherical model. It is shown that the off-center spherical model yields scaling ratios, in the brain tissue, which lie between the extreme values predicted by the concentric and isolated spherical models.

This report was submitted in fulfillment of Contract 68-02-4092 by the University of Miami under the sponsorship of the U.S. Environmental Protection Agency. This report covers the period July 17, 1984 to January 17, 1985.

SECTION 1

INTRODUCTION

A problem of considerable importance to the understanding of biological phenomena produced by electromagnetic radiation, is the mechanism of interaction of amplitude-modulated radio-frequency [RF] waves on calcium-ion efflux from in vitro chick brain [Bawin et al., 1975; Blackman et al., 1979, 1980a, 1980b, 1981 and 1985; Sheppard et al., 1979]. These works have demonstrated that RF radiation, when amplitude modulated with extremely low frequency [ELF] sinusoidal waves, can enhance the calcium-ion efflux from in vitro chick brain tissue.

The calcium-ion efflux phenomena has several interesting aspects. It occurs only when the RF carrier wave is amplitude modulated at ELF. The peak effect occurs with 16 Hz amplitude-modulated RF fields, and no effect is observed with unmodulated RF carrier waves, or with modulation frequencies below 6 Hz or above 50 Hz. The calcium-ion efflux occurs at only certain electric field intensities in the chick brain. Joines and Blackman [1980] have shown that the effect also occurs at other carrier frequencies if the average electric field intensity in the chick brain remains the same. That is, if the incident power density is adjusted by an amount that compensates for the change in frequency and complex permittivity of the chick brain.

In order to better understand the effects of amplitude-modulated RF radiation on calcium-ion efflux, the electromagnetic fields and absorbed power density distribution in the chick brain must be accurately determined. Concentric spherical models [Joines and Blackman, 1980, 1981; Joines et al., 1981] have been developed to calculate the field and power density distribution in the chick brain. These models have provided much valuable information about the dosimetric aspects of the calcium-ion efflux experiments. The models have also been used to develop scaling ratios to determine the required incident power density that produces calcium-ion efflux at other carrier frequencies.

This study overcomes the limitations of the concentric spherical models. Concentric spherical models do not adequately represent the chick brain half immersed in the buffer medium, because the brain as it sits in the bottom of the test tube is surrounded by a layer of buffer solution with a thickness that is different above and below the brain. Concentric spherical models use a uniform layer of buffer solution to surround the brain. To determine the dosimetric effects of the non-uniform layer, an

off-center spherical model is used to approximate the physical geometry of the brain/buffer combination. The off-center spherical model represents a significant refinement to the concentric spherical model since the brain can be modeled as a continuous, smooth, spherical surface surrounded by unequal amounts of buffer solution on its upper and lower surfaces. The electric field and absorbed power density distributions, and scaling ratios for carrier waves of 50, 100, and 147 MHz are calculated using a quasi-static approximation. This approximation leads to a field representation in terms of a convergent series involving spherical harmonics.

SECTION 2

THEORETICAL RESULTS

The schematic of the experimental set-up [see Blackman et al., 1981] is shown in Fig. 1. The chick brain tissue sits at the bottom of the test tube and it is surrounded by a non-uniform layer of buffer solution. The hemispherical bottom of the test tube has an inner radius of 0.71 cm. The chick brain has a mean horizontal dimension of 1 cm and a mean height of 0.81 cm. The mean height from the top of the tissue to the surface of the buffer solution is 0.24 cm.

The analytical model for the off-center spherical model of the brain inside a test tube is shown in Fig. 2, along with the direction of the incident electric field. This model represents the geometry in Fig. 1. In fact, except for the flat-topped buffer region the model is reasonably accurate. The radii a and b, and the off center distance d, are selected so that the brain volume occupies 0.3 ml, and the buffer volume 1 ml. Also, the limiting case as h approaches zero is analyzed.

The mathematical formulation that follows is by no means a simple extension of the concentric spherical case. To the best of the authors' knowledge exact solutions to off-center spherical geometries, of the type shown in Fig. 2, in terms of zonal harmonic expansions have not appeared in the literature. A simpler problem involving an off-center spherical capacitor is given in Morse and Feshbach [1953], together with an ingenious set of expansions that permits the closed form solution of some off-center spherical problems.

The mathematical formulation of the problem follows. The electric field, assuming quasi-static conditions, can be expressed as

$$\underset{\sim}{E} = -\nabla\phi$$

where ϕ is the electrostatic potential. The quasi-static approximation is valid because of the dimensions, frequencies and electrical properties of the materials involved. In our calculations, the relative complex permittivity (K) of the brain tissue at the typical carrier frequencies used in calcium-ion studies are 100-j175 at 50 MHz, 72-j94.9 at 100 MHz, and 66-j69.2 at 147 MHz; for the buffer the values are 71-j580 at 50 MHz, 71-j290 at 100 MHz, and 71-j200 at 147 MHz [Hollis et al., 1980]. The relative complex permittivity is defined by

$$K = \frac{\sigma + j\omega\varepsilon}{j\omega\varepsilon_o}$$

The externally applied field, which makes an angle of 90° with the x-axis (i.e., $\underset{\sim}{E}=E_o u_y$) produces a potential which can be expressed in spherical coordinates in the form

$$V_{ext} = -E_o r_a Y_{11}^e(\theta_a, \phi)$$

or

$$V_{ext} = -E_o r_b Y_{11}^e(\theta_b, \phi)$$

where

$$Y_{nm}^e(\theta, \phi) = \cos m\phi \; P_n^m(\cos\theta)$$

The associated Legendre polynomials $P_n^m(\cos\theta)$ are defined as [Morse and Feshbach, 1953]

$$P_n^m(x) = (1-x^2)^{m/2} \frac{d^m}{dx^m} P_n(x)$$

where $P_n(x)$ are Legendre polynomials.

The potential in regions I, II and III satisfies Poisson's equation, subject to the appropriate boundary conditions. The charge distributions at $r_a = a$ and $r_b = b$ produce potentials V_a and V_b of the form

$$V_a = \begin{cases} V_{a,in} = \sum_{n=0}^{\infty}\sum_{m=0}^{n} \alpha_{nm} \left(\frac{r_a}{a}\right)^n Y_{nm}^e(\theta_a, \phi) & (r_a \leq a) \\ V_{a,out} = \sum_{n=0}^{\infty}\sum_{m=0}^{n} \alpha_{nm} \left(\frac{a}{r_a}\right)^{n+1} Y_{nm}^e(\theta_a, \phi) & (r_a \geq a) \end{cases} \tag{1}$$

and

$$V_b = \begin{cases} V_{b,in} = \sum_{n=0}^{\infty}\sum_{m=0}^{\infty} \beta_{nm} \left(\frac{r_b}{b}\right)^n Y_{nm}^e(\theta_b, \phi) & (r_b \leq b) \\ V_{b,out} = \sum_{n=0}^{\infty}\sum_{m=0}^{n} \beta_{nm} \left(\frac{b}{r_b}\right)^{n+1} Y_{nm}^e(\theta_b, \phi) & (r_b \geq b) \end{cases} \tag{2}$$

where α_{nm} and β_{nm} are constants to be determined from the boundary conditions. In terms of (1) and (2), the potentials in the three regions are given by

$$V_I = V_{a,in} + V_{b,out} + V_{ext} \tag{3}$$

$$V_{II} = V_{a,out} + V_{b,out} + V_{ext} \tag{4}$$

$$V_{III} = V_{a,in} + V_{b,in} + V_{ext} \tag{5}$$

The form selected for the potentials in (1) and (2) satisfy the continuity conditions at $r_a = a$ and $r_b = b$. Therefore, the boundary conditions that remain to be satisfied at the interface are the continuity of the normal component of the current density at $r_a = a$ and $r_b = b$, namely

$$(\sigma_1 + j\omega\varepsilon_1)\frac{\partial V_I}{\partial r_a}\Big]_{r_a=a} = j\omega\varepsilon_2\frac{\partial V_{II}}{\partial r_a}\Big]_{r_a=a} \tag{6}$$

and

$$(\sigma_1 + j\omega\varepsilon_1)\frac{\partial V_I}{\partial r_b}\Big]_{r_b=b} = (\sigma_3 + j\omega\varepsilon_3)\frac{\partial V_{III}}{\partial r_a}\Big]_{r_b=b} \tag{7}$$

In order to apply the boundary conditions at the surface of the off-center sphere (i.e., at $r_b = b$), we need to expand the solution $V_{a,in}$ in terms of the coordinates r_b, θ_b and ϕ, and the solution $V_{b,out}$ in terms of the coordinates r_a, θ_a, and ϕ. The necessary expansions are [Morse and Feshbach, 1953]

$$V_{a,in} = \sum_{n=0}^{\infty}\sum_{m=0}^{n}\alpha_{nm}a^{-n}\sum_{s=m}^{n}f_{snm}r_b^s\,Y_{sm}^e(\theta_b,\phi) \tag{8}$$

and

$$V_{b,out} = \sum_{n=0}^{\infty}\sum_{m=0}^{n}\beta_{nm}b^{n+1}\sum_{s=m}^{n}g_{snm}r_a^{-s-1}\,Y_{sm}^e(\theta_a,\phi) \tag{9}$$

where

$$f_{snm} = \frac{(-1)^{n-s}(n+m)!\,d^{n-s}}{(n-s)!\,(s+m)!}$$

and

$$g_{snm} = \frac{d^{s-n}(s-m)!}{(n-m)!\,(s-n)!}$$

Substituting (3), (4) and (5) into (6) and (7), and using (8) and (9), we obtain the following set of linear equations for the $n=j$ ($j=0,1,\ldots$) and $m=k$ ($k=0,1,\ldots,n$) coefficients (i.e., α_{jk} and β_{jk}):

$$E_o(1-K_1)\delta_{j,1}\delta_{k,1} + \frac{1}{a}\alpha_{jk}[(j+1) + jK_1]$$

$$+ \sum_{v=k}^{j}\beta_{vk}(1-K_1)\frac{(-1)^{j-v}(j-k)!\,(j+1)b^{v+1}d^{j-v}}{(v-k)!\,(j-v)!\,a^{j+2}} = 0 \tag{10}$$

and

$$E_o(1-K_3)\delta_{j,1}\delta_{k,1} + \frac{1}{b}\beta_{jk}[(j+1) + jK_3]$$

$$+ \sum_{v=j}^{\infty} \alpha_{vk}(K_3-1)\frac{(-1)^{v-j}(v+k)!jb^{j-1}d^{v-j}}{(v-j)!(j+k)!a^v} = 0 \qquad (11)$$

where

$$K_1 = \frac{\sigma_1 + j\omega\varepsilon_1}{j\omega\varepsilon_o}$$

and

$$K_3 = \frac{\sigma_3 + j\omega\varepsilon_3}{j\omega\varepsilon_o}$$

Fixing the maximum n to be N_{max}, (10) and (11) result in $2N_{max}$ unknowns for each value of m. Only m=k=1 contributes because the equations are linear and the right hand side is zero for m>1. These equations are solved for α_{j1} and β_{j1}, j=0 to N_{max}, and the results are then inserted into (1) to (5) to calculate the potential in the three regions.

The electric field and power density distributions are calculated as follows. The x-component of the electric field is found by numerical differentiation:

$$E_x(x,y,z) \approx [\phi(x+\Delta x,y,z) - \phi(x-\Delta x,y,z)]/2\Delta x$$

and the same for the other components. The time average absorbed power density is then determined according to $\sigma|\underline{E}|^2/2$.

A computer program was written to calculate the field and absorbed power density distribution in the brain/buffer regions. The listing of the program, including a description, is given in Appendix A.

The absorbed power density distributions, assuming E_o=1 V/m, were calculated for several cases, the most important was for a brain volume of 0.3 cm^3, buffer volume of 1 cm^3, and h=0.05 cm. Therefore, a=0.677 cm, b=0.415 cm, d=0.212 cm, and t=0.474 cm. Also, the limiting cases as h approaches zero, and d approaches zero are considered. For $h \rightarrow 0$ (i.e., when the spheres touch at the bottom) the dimensions are a=0.677 cm, b=0.415 cm, d=0.262 cm, and t=0.524 cm.

Figs. 3 and 4 illustrate graphically the absorbed power density distribution produced by an incident carrier wave at

50 MHz for the cases where h=0.05 cm and d $\rightarrow$ 0, respectively. Figs. 5 to 8 give the results at 100 MHz and 147 MHz. Each line in the figures represents a constant absorbed power density level. The number scale is linear, ranging from 0 to 9, where 9 represents a power density of 0.083 mW/m^3 at 50 MHz, 0.3 mW/m^3 at 100 MHz, and 0.5 mW/m^3 at 147 MHz. For example, the value of 2 in Fig. 7 represents a absorbed power density of (2/9)0.5=0.111 mw/m^3. Also, there are two constant (unlabeled) power density lines between the labeled lines. Each of these lines represents an increment of 1/3. For example, the two lines between 3 and 4, represent 3 1/3 and 3 2/3. In the brain region the absorbed power density increases toward the bottom. For example in Fig. 7, the absorbed power density level varies from a value of 2 toward the top to 2 2/3 toward the bottom. In Figs. 4, 6, and 8 the absorbed power density distribution in the brain region is constant at the values of 0.0143 mW/m^3 at 50 MHz, 0.0547 mW/m^3 at 100 MHz, and 0.109 mW/m^3 at 147 MHz.

The limiting case as h $\rightarrow$ 0 was also calculated, and the values of the absorbed power density used in the calculations of the scaling ratios. The absorbed power density profile was essentially the same as that for the h=0.05 cm case (see Fig. 3), except the values toward the bottom are somewhat larger.

The power density distribution was also calculated for the case of a brain volume of 0.3 cm^3, t=0.24 cm, and h=0.05 cm. In this case a=0.56 cm, b=0.415 cm and d=0.095 cm. The absorbed power density distribution is similar to those in Figs. 3 to 8. Fig. 9 illustrates the power density distribution at 147 MHz for this case.

From Figs. 3 to 9 it is seen that the absorbed power levels are larger at higher frequencies. This is a result of the brain tissue becoming more conductive as the frequency increases.

It is significant to observe from Figs. 3, 5, 7, and 9 that the absorbed power density distribution is not uniform, the bottom of the chick brain has higher absorbed power densities. Also, the surface fields around the chick brain exhibit a significant variation from the bottom to the top. These results are somewhat different from those predicted by the concentric spherical model in Fig. 5 [see also Joines and Blackman, 1981].

SECTION 3

SCALING RELATIONS

It has been shown [Joines and Blackman, 1981] that by maintaining a constant average electric field within the brain tissue, calcium-ion efflux results at one frequency can be used to extrapolate those at another frequency. It is therefore important to be able to determine what incident power densities are required to maintain a constant internal electric field as the frequency of the electromagnetic field changes. The necessary scaling relations can be determined by writing the internal electric field as

$$|\underset{\sim}{E}|^2 = |\underset{\sim}{E}_i|^2 F \tag{12}$$

where F is related to the electromagnetic absorptive properties of the brain and $\underset{\sim}{E}_i$ is the incident electric field. The incident field is related to the incident power density according to

$$P_i = |\underset{\sim}{E}_i|^2 / 2\eta_o \tag{13}$$

where η_o=377 ohms is the intrinsic impedance of free space. Substituting (13) into (12) and forming the ratio between the internal electric field at two different frequencies yields the following relation

$$\frac{P_i(f_1)}{P_i(f_2)} = \frac{|\underset{\sim}{E}(f_1)|^2}{|\underset{\sim}{E}(f_2)|^2} \cdot \frac{F(f_2)}{F(f_1)}$$

where f_1 denotes the frequency considered. Requiring a constant internal electric field means that

$$|\underset{\sim}{E}(f_1)| = |\underset{\sim}{E}(f_2)|$$

Therefore,

$$\frac{P_i(f_1)}{P_i(f_2)} = \frac{F(f_2)}{F(f_1)} \tag{14}$$

In order to determine values for (14), it is necessary to consider the power absorbed and express it in the form

$$P_a(f) = \tfrac{1}{2}\sigma |\underset{\sim}{E}_i|^2 F(f)$$

At $f=f_1$, we can determine $P_a(f_1)$ for $E_1=1$ V/m then $F(f_1)$ follows. Similarly, at $f=f_2$, we can determine $P_a(f_2)$ and $F(f_2)$ follows. If these values are inserted into (14), the scaling ratios can be determined.

Figs. 10 and 11 give the values of the scaling ratios that make the electric field intensity the same at f_1 and f_2 for points along the z-axis inside the spherical brain between the top (i.e., z=0.415 cm) and bottom (i.e., z=-0.415 cm).

Figs. 12 and 13 give values of the scaling factors that make the electric field intensity the same at f_1 and f_2 for points on the outside surface of the brain between the top (i.e., $\theta=0$) and bottom (i.e., $\theta=\pi$) for $0\leq\theta\leq\pi$.

Some interesting observations can be made from Figs. 10 to 13. The scaling ratios at a given frequency are continuous at the top and bottom of the brain-buffer interface. This follows from the fact that electric field is tangential and continuous at the top and bottom brain-buffer interface. For example, at z=0.415 cm in Fig. 10 the scaling ratio is 3.56, which is similar to the scaling ratio at $\theta=0$ in Fig. 12. The scaling ratio in the concentric spherical case (i.e., when d=0) is constant in the brain region at the value of 3.56 in Fig. 10, and 6.57 in Fig. 12. The scaling ratio value of 6.57 for $P_i(50)/P_i(147)$ compares favorably with the one obtained by Joines and Blackmrn [1981], namely 6.6.

SECTION 4

CONCLUSIONS

The off-center spherical model was used to calculate the electric field and absorbed power density distribution in chick brain tissue inside a test tube. The calculations were made with typical dielectric data used in previous analytical studies for carrier frequencies of 50 MHz, 100 MHz and 147 MHz. In the experimentally realistic case where the chick brain is surrounded by lesser amounts of buffer solution at the bottom, the pattern of absorbed power densities was found to show a marked concentration of absorbed power near the bottom. The absorbed power density within the brain showed only gradual variations with position. Outside, at the surface of the brain, the absorbed power density distribution varied by factors of 6 to 10.

The scaling ratios were calculated as a function of position for points inside, and on the outside surface of the brain. The off-center spherical model revealed that the scaling ratio inside the brain tissue is not constant; the maximum change (h=0 case) from the top of the brain to the bottom was approximately 11% for $P_i(50)/P_i(100)$, and 19% for $P_i(50)/P_i(147)$. This is in contrast to the concentric spherical model which predicts no change. As would be expected, the scaling ratios near the top are essentially identical to the values predicted by the concentric spherical model; at the bottom the values become closer to those predicted by an isolated spherical model. Thus, the off-center spherical model yields internal scaling ratios which lie between the extreme values predicted by the concentric and isolated spherical models.

Recent experimental studies [Blackman and Wilson, 1983; Adey et al., 1982] have shown that the penetration of radioactive calcium-ions in chick brain tissue was no greater than 1 mm from the surface. Thus, it may be concluded that surface field values are of paramount importance. The profiles for the surface scaling ratios are symmetric for the concentric spherical case, with the peak value occurring at a point on the surface ($\theta=90°$), where the external electric field is normal to the surface. However, the off-center spherical model yielded somewhat lower peak values whose position shifted toward the bottom ($\theta\approx99°$). In addition, the surface ratios were similar at the top of the brain for all the models, but the values at the bottom varied considerably, with the h=0 case approaching the value given for an isolated sphere.

The scaling ratio results have provided new insights into

the interpretation of the calcium-ion efflux phenomena. The information presented in this study can be used by the experimentalists in the interpretation of their results, and in the formulation of theories concerning the calcium-ion efflux phenomena.

REFERENCES

Adey W.R, S.M. Bawin,and A.F. Lawrence (1982): Effects of weak amplitude-modulated microwave fields on calcium efflux from awake cat cerebral cortex. Bioelectromagnetics 3:295-307.

Bawin S.M., L.K. Kaczmark, and W.R. Adey (1975): Effects of modulated VHF fields on the central nervous system. ANN NY ACAD SCI 247, 247-81.

Blackman C.F., J.A. Elder, C.M. Weil, S.G. Benane, D.C. Eichinger, and D.E. House (1979): Induction of calcium-ion efflux from brain tissue by radio-frequency radiation: Effects of modulation frequency and field strength. Radio Science 14(6S), 93-98.

Blackman C.F., S.G. Benane, J.A. Elder, D.E. House, J.A. Lampe, and J.M. Faulk (1980a): Induction of calcium-ion efflux from brain tissue by radio-frequency radiation: Effect of sample number and modulation frequency on the power-density window. Bioelectromagnetics 1:35-43.

Blackman, C.F., S.G. Benane, W.T. Joines, M.A. Hollis and D. E. House (1980b): Calcium-ion efflux from brain tissue: Power density vs. internal field intensity dependencies at 50 MHz RF radiation. Bioelectromagnetics 1, 277-283.

Blackman, C.F., W.T. Joines and J.A. Elder (1981): Calcium-ion efflux in brain tissue by radiofrequency radiation. Biological Effects of Nonionizing Radiation (K. H. Illinger, Ed.), ACS Symposium Series (American Chemical Society, Washington, D.C.), No. 157, 299-314.

Blackman C.F., and B.S. Wilson (1983): Distribution of label in studies on the effects of nonionizing radiation on the association of calcium-ions with brain tissue. Abstract #GJ-24, 5th Annual Scientific Session, The Bioelectromagnetics Society, 12-17 July, Boulder, CO (available from The Bioelectromagnetics Society, One Bank Street, Suite 307, Gaithersburg, Maryland 20878), 73.

Blackman CF, Benane SG, House DE, and Joines WT (1985): Effects of ELF (1-120 Hz) and modulated (50 Hz) RF fields on the efflux of calcium ions from brain tissue in vitro. Bioelectromagnetics 6: 1-11.

Hollis, M.A., C.F. Blackman, C.M. Weil, J.R. Allis and D. J. Schaefer (1980): A swept-frequency magnitude method for the dielectric characterization of chemical and biological systems.

IEEE Trans. Microwave Theory Tech., MTT-28, 791-801.

Joines W.T.and C.F. Blackman (1980): Power density, field intensity, and carrier frequency determinants of RF-energy-induced calcium-ion efflux from brain tissue. Bioelectromagnetics 1, 271-275.

Joines, W.T., C.F. Blackman, and M.T. Hollis (1981): Broadening of the RF power-density window for calcium-ion efflux from brain tissue, IEEE Trans. on Biomedical Engineering, No.8, 568-573.

Joines, W.T. and C. F. Blackman (1981): Equalizing the electric field intensity within chick brain immersed in buffer solution at different carrier frequencies, Bioelectromagnetics 2, 411-413.

Morse, P.M. and H. Feshbach (1953): Methods of Theoretical Physics, McGraw-Hill Co. New York.

Sheppard A.R., S.M. Bawin, and W.R. Adey (1979): Models of long-range order in cerebral macromolecules: Effects of sub-ELF and modulated VHF and UHF fields. Radio Science 14 (65), 141-145.

APPENDIX A

COMPUTER PROGRAM

This computer program was written in Fortran-77, and should run in standard computers with FORTRAN compilers.

The program consist of a main program, called DOPOWER, two subroutines (SETMAT and LGNDRE), and two functions (POTENT and POWER), and requires the IMSL mathematical subroutine LEQT1C. The subroutine LEQT1C must be run using double precision real and complex variables. Each program is described in the comments.

In a typical run the program requests the value of the parameters a, b, d and angle, where angle is the angle of inclination of the electric field with the z-axis (i.e., θ). Also, the values of the relative dielectric constants K_1 and K_2 are requested, followed by the values of the conductivities. Then, the program calculates the value of the absorbed power density at given values of y and z.

A computer program that does the calculations and the plotting of the power density distribution, as shown in Figs. 3 to 9, is available from the authors. This program will run with a Vectrix graphics display, or a H. P. 7475A plotter.

PROGRAM LISTING

```
C     PROGRAM DOPOWER
      PARAMETER ( NORDER = 8 , NCOEFF = 2*NORDER )
      PARAMETER ( NPOTST = 54 , NDIMOT = 400 )

C     THE MAIN CALLING ROUTINE TO COMPUTE THE POWERS FOR THE
C     NON-CONCENTRIC SPHERE PROBLEM.

C     1: READ THE PARAMETERS TO DESCRIBE THE GEOMETRY OF THE SPHERES
C        AND TO FIX THE DIELECTRIC PROPERTIES OF THE SPHERES.

C     2: SET UP THE MATRIX TO DETERMINE THE COEFFICIENTS OF THE
C        EXPANSION IN LEGENDRE POLYNOMIALS.  NOTE: THIS CALCULATION
C        ASSUMES THAT THE EXTERNAL ELECTRIC FIELD IS AZIMUTHALLY SYMMETRIC.

C     3: CALL THE IMSL ROUTINE LEQT1C TO SOLVE THE MATRIX EQUATION
C        RELATING THE COEFFICIENTS OF THE EXPANSION TO THE APPLIED EXTERNAL
C        FIELD. THE CALCULATIONS IN LEQT1C MUST BE DONE IN DOUBLE PRECISION.
```

```
C     4: USE THESE COEFFICIENTS AS INPUT TO THE POTENTIAL FUNCTION CALCULATOR.
C        THIS IS A COMPLEX VALUED FUNCTION THAT GIVES THE COMPLEX POTENTIAL.

C        NOTE:  THE EXTRANEOUS VARIABLES ARE PASSED THROUGH COMMON.

      IMPLICIT DOUBLE PRECISION ( A-H , O-Z )
      COMPLEX*16 DIEL1 , DIEL3 , COEFF( NCOEFF , 0:1 )
     *         , XMAT( NCOEFF , NCOEFF , 0:1 )
      DIMENSION WA ( NCOEFF )

9     FORMAT ( A40 )

      EXTERNAL POT , STOPFN , POTLIN , POWER , POWDIV , POTLIM , POTIM
      COMMON /ABDCO/ A , B , D , THETA0 , COEFF
      COMMON /CONDUC/ SIGMA1 , SIGMA3

      PRINT*, 'THE GEOMETRY: A , B , D (METERS) , ANGLE(DEGREES)'
      READ*, A , B , D , THDEG
      THETA0 = THDEG*3.141592/180.

      PRINT*,'THE DIELECTRIC CONSTANTS, K1 AND K3'
      READ*, DIEL1 , DIEL3
      DIEL3 = DIEL3/DIEL1

      PRINT*, 'THE CONDUCTIVITIES, SIGMA1 AND SIGMA3'
      READ*, SIGMA1 , SIGMA3

      CALL SETMAT ( XMAT , NCOEFF , DIEL1 , DIEL3 , A , B , D )

      COEFF( 1 , 0 ) = ( DIEL1 - 1. )*COS( THETA0 )
      COEFF( 2 , 0 ) = ( 1. - DIEL3 )*COS( THETA0 )
      COEFF( 1 , 1 ) = ( DIEL1 - 1. )*SIN( THETA0 )
      COEFF( 2 , 1 ) = ( 1. - DIEL3 )*SIN( THETA0 )

      DO 50 M = 0 , 1
         CALL LEQT1C ( XMAT( 1 , 1 , M ) , NCOEFF , NCOEFF
     *         , COEFF( 1 , M ) , 1 , NCOEFF , 0 , WA , IER )
50    CONTINUE

      PRINT*, 'ENTER Y AND Z COORDINATES'

C     DO FOREVER
9999  CONTINUE
         READ ( 5 , * , END=10000 ) Y , Z
         PRINT*, POWER( Y , Z ) , ' WATTS/METER CUBED'
      GO TO 9999
C     END FOREVER

10000 CONTINUE
      END
```

****

```
C     THIS SUBROUTINE INITIALIZES THE MAIN MATRIX FOR THE
C     NON-CONCENTRIC SPHERICAL PROBLEM.  IT ASSUMES AZIMUTHAL SYMMETRY.
C     THE DIMENSIONS OF THE SPHERES ARE:
C                 A = RADIUS OF THE OUTER SPHERE
C                 B = RADIUS OF THE INNER SPHERE
C                 D = THE DISTANCE BETWEEN THE CENTERS

C     THE (COMPLEX) DIELECTRIC FOR THE OUTER SPHERE IS DIEL1.
C     THE RATIO OF THE INNER DIELECTRIC TO THE OUTER IS DIEL3.

C     THE SIZE OF THE MATRIX IS  N2 BY N2.  THE MAXIMUM HARMONIC
C     KEPT IS  EXACTLY ONE-HALF OF THIS.

C     M IS THE AZIMUTHAL VARIABLE.  IT IS EITHER 0 OR 1.

C     THE MATRIX IS BLOCKED SO THAT BOTH THE OUTER AND THE INNER
C     COEFFICIENTS ARE TOGETHER.  I.E. THE COLUMN MATRIX ON WHICH
C     THIS IS TO ACT IS ARRANGED AS:

C           A1 , B1 , A2 , B2 , ... , AN , BN

      SUBROUTINE SETMAT ( XMAT , N2 , DIEL1 , DIEL3 , A , B , D )

      IMPLICIT DOUBLE PRECISION ( A-H , O-Z )
      COMPLEX*16 DIEL1 , DIEL3 , XMAT
      DIMENSION XMAT ( N2 , N2 , 0:1 )

      IF ( MOD( N2 , 2 ) .NE. 0 ) THEN
         PRINT*, 'THE MATRIX MUST HAVE AN EVEN DIMENSION.  '
         STOP
      ENDIF

      N = N2/2

C     THE DIAGONAL ELEMENTS ARE HANDLED DIRECTLY.  (NOTE THAT THE
C     MATRIX IS ASSUMED TO HAVE BEEN ZEROED INITIALLY.)

      DO 500 M = 0 , 1
         DO 100 I = 1 , N2 , 2
            K = ( I + 1 )/2
            XMAT ( I , I , M ) = ( K + 1. + K*DIEL1 )/A
100      CONTINUE

         DO 200 I = 2 , N2 , 2
            K = I/2
            XMAT ( I , I , M ) = - ( K + 1. + K*DIEL3 )/B
200      CONTINUE

C        THE ABOVE ELEMENTS DID NOT CONNECT ANY UNKNOWN TO ANY OTHER.
C        THE NEXT WILL FILL IN THE LOWER TRIANGLE OF THE MATRIX.
```

```
C       THE FIRST INDEX ( I ) DESIGNATES THE ROWS, AND  J THE COLUMNS

        DO 300 I = 1 , N
           DO 300 J = 1 , I

              XMAT ( 2*I - 1 , 2*J , M ) =  ( (-1)**( I - J ) )*
     *         ( GAMMA( I + 1 - M )*( I + 1)/
     *         ( GAMMA( J + 1 - M )*GAMMA( I - J + 1 ) ) )*
     *         ( D**( I - J ) )*( B**( J + 1 )/( A**( I + 2 ) ) )*
     *         ( 1. - DIEL1 )

300     CONTINUE

C       NOW FOR THE UPPER TRIANGLE

        DO 400 I = 1 , N
           DO 400 J = I , N

              XMAT ( 2*I , 2*J - 1 , M ) = ( (-1)**( I - J ) )*
     *          ( GAMMA( J + 1 + M )*I/
     *         ( GAMMA( J - I + 1 )*GAMMA( I + 1 + M ) ) )*
     *         ( ( D**( J - I ) )*( B**( I - 1 ) )/( A**J ) )*
     *         ( 1. - DIEL3 )

400     CONTINUE

500   CONTINUE

      RETURN
      END

                ***********************************************

      COMPLEX FUNCTION POTENT*16 ( X , Y , A , B , D , THETA0 , COEFF )
      PARAMETER ( NORDER = 8 , NCOEFF = 2*NORDER )

C     COMPUTE THE POTENTIAL FUNCTION FOR THE OFF-CENTER CONCENTRIC
C     SPHERICAL PROBLEM.  THE INPUT COORDINATES ARE GIVEN IN
C     RECTANGULAR COORDINATES.
C     THE RADII OF THE SPHERES ARE A (OUTER) AND B (INNER).  THE DISTANCE
C     BETWEEN CENTERS IS D.
C     NORDER IS THE NUMBER OF TERMS KEPT IN THE LEGENDRE POLYNOMIAL
C     EXPANSION OF THE POTENTIAL, AND THE COEFFICIENTS OF THE EXPANSION
C     ARE GIVEN IN THE ARRAY COEFF.

      IMPLICIT DOUBLE PRECISION ( A-H , O-Z )
      COMPLEX*16 VEXT , COEFF( NCOEFF , 0:1 )
      DIMENSION ALEGND( 0:NORDER , 0:1 ) , BLEGND( 0:NORDER , 0:1 )

C     FIRST DO ALL OF THE GEOMETRY: FROM X AND Y, GET THE TWO SPHERICAL
C     SETS OF COORDINATES.
```

```
      RA = SQRT( X*X + Y*Y )
      COSTH = Y/RA
      SINTH = X/RA
      RB = SQRT( X*X + ( Y + D )*( Y + D ) )
      COSTHB = ( Y + D )/RB
      IF ( X .GE. 0. ) THEN
         SIGNUM = 1.
         ELSE
         SIGNUM = -1.
      ENDIF

      CALL LGNDRE( NORDER , COSTH , ALEGND )
      CALL LGNDRE( NORDER , COSTHB , BLEGND )

      VEXT = -RA*( COSTH*COS( THETA0 )
     *             + SINTH*SIN( THETA0 ) )

      IF ( RA .GE. A ) THEN
         RATIOA = A/RA
         DENOMA = RATIOA**2
      ELSE
         RATIOA = RA/A
         DENOMA = RATIOA
      ENDIF

      IF ( RB .GE. B ) THEN
         RATIOB = B/RB
         DENOMB = RATIOB**2
      ELSE
         RATIOB = RB/B
         DENOMB = RATIOB
      ENDIF

      DO 300 M = 0 , 1
         S = SIGNUM**M

         DMA = DENOMA
         DO 100 I = 1 , NORDER
            VEXT = VEXT + COEFF( 2*I - 1 , M )*ALEGND( I , M  )*DMA*S
            DMA = DMA*RATIOA
100      CONTINUE

         DMB = DENOMB
         DO 200 I = 1 , NORDER
            VEXT = VEXT + COEFF( 2*I , M )*BLEGND( I , M  )*DMB*S
            DMB = DMB*RATIOB
200      CONTINUE
300   CONTINUE

      POTENT = VEXT
      RETURN
      END
```

```
*************************************************

      DOUBLE PRECISION FUNCTION POWER( X, Y )
      PARAMETER ( NORDER = 8 , NCOEFF = 2*NORDER )

C     THE POWER DENSITY AS COMPUTED FROM THE COMPLEX POTENTIAL FUNCTION
C     POTENT.
C     AT THE BOUNDARIES, THE ALGORITHM IS CHANGED SO THAT THE
C     DIFFERENCE QUOTIENT STAYS ON THE CORRECT SIDE OF THE
C     INTERFACE.

      IMPLICIT DOUBLE PRECISION ( A-H , O-Z )
      COMMON /ABDCO/ A , B , D , THETA0 , COEFF
      COMMON /CONDUC/ SIGMA1 , SIGMA3

      COMPLEX*16 COEFF( NCOEFF , 0:1 ) , POTENT , DIFF
      EXTERNAL POTENT
      DIMENSION RT( -1:1 , -1:1 , 0:1 ), DEL( -1:1 , -1:1 ), RAD( 0:1 )
      DIMENSION SPHERE( 0:1 )

C     THE MATRIX RT IS USED TO HOLD THE DISTANCES OF THE FOUR COORDINATES
C     USED TO COMPUTE THE DERIVATIVES (FROM THE TWO ORIGINS, THAT IS).
C     IF THESE DISTANCES CROSS A BOUNDARY, THE DIFFERENTIATION
C     ALGORITHM MUST CHANGE.

      DELTA = .0001*A
      RAD( 0 ) = SQRT( X*X + Y*Y )
      RAD( 1 ) = SQRT( X*X + ( Y + D )*( Y + D ) )
      SPHERE( 0 ) = A
      SPHERE( 1 ) = B

      DO 30 I = -1 , 1
         DO 20 J = -1 , 1
            DO 10 K = 0 , 1
               RT( I , J , K ) =
     *            SQRT( ( X + I*DELTA )**2 + ( Y + J*DELTA + K*D )**2 )
10          CONTINUE
20       CONTINUE
30    CONTINUE

      DEL( -1 , 0 ) = DELTA
      DEL( 1 , 0 ) = DELTA
      DEL( 0 , -1 ) = DELTA
      DEL( 0 , 1 ) = DELTA

      DO 100 K = 0 , 1
         DR = RAD( K ) - SPHERE( K )

         IF ( DR .EQ. 0. ) THEN
            DEL( -1 , 0 ) = 0.
            DEL( 0 , -1 ) = 0.
```

```
         ELSE
            DO 50 I = -1 , 1 , 2
               IF ( DR*( RT( I , 0 , K ) - SPHERE( K ) ) .LT. 0. )
     *                 DEL( I , 0 ) = 0.
50          CONTINUE

            DO 60 J = -1 , 1 , 2
               IF ( DR*( RT( 0 , J , K ) - SPHERE( K ) ) .LT. 0. )
     *                 DEL( 0 , J ) = 0.
60          CONTINUE

         ENDIF
100   CONTINUE

      DIFF=POTENT( X + DEL( 1 , 0 ) , Y , A , B , D , THETA0 , COEFF ) -
     *      POTENT( X - DEL( -1 , 0 ) , Y , A , B , D , THETA0 , COEFF )
      POW = DIFF*CONJG( DIFF )/( ( DEL( 1 , 0 ) + DEL( -1 , 0 ) )**2 )

      DIFF=POTENT( X , Y + DEL( 0 , 1 ) , A , B , D , THETA0 , COEFF ) -
     *      POTENT( X , Y - DEL( 0 , -1 ) , A , B , D , THETA0 , COEFF )
      POW = POW
     *    + DIFF*CONJG( DIFF )/( ( DEL( 0 , 1 ) + DEL( 0 , -1 ) )**2 )

      IF ( RAD( 0 ) .GE. A ) THEN
         SIGMA = 0.

      ELSE IF ( RAD( 1 ) .GE. B ) THEN
         SIGMA = SIGMA1                    SIGMA = SIGMA1

      ELSE
         SIGMA = SIGMA3
      ENDIF

      POWER = SIGMA*POW/2.

      RETURN
      END

                  **********************************************

C     COMPUTE THE LEGENDRE FUNCTIONS OF ARGUMENT X.
C     USE THE UPWARD RECURSION RELATION OF ABRAMOWITZ AND STEGUN
C     CHAPTER 22:  22.7.10
C     THE INPUT VARIABLE MAXORD SPECIFIES THE MAXIMUM ORDER OF THE
C     LEGENDRE POLYNOMIAL TO BE COMPUTED.  THE RESULT IS IN ARRAY OUTPUT.
C
C     THE OUTPUT IS AN ARRAY OF DIMENSION MAXORD BY 2.
C     IT CONTAINS THE VALUES OF P-NM.

      SUBROUTINE LGNDRE ( MAXORD , X , OUTPUT )
```

```
      IMPLICIT DOUBLE PRECISION ( A-H , O-Z )
      DIMENSION OUTPUT( 0:MAXORD , 0:1 )

      OUTPUT( 0 , 0 ) = 1.
      OUTPUT( 1 , 0 ) = X
      OUTPUT( 0 , 1 ) = 0.
      OUTPUT( 1 , 1 ) = SQRT( 1. - X*X )

      DO 20 M = 0 , 1
         DO 10 I = 1 , MAXORD - 1
            OUTPUT( I+1 , M ) = ( ( 2*I + 1 )*X*OUTPUT( I , M )
     *                  - ( I + M )*OUTPUT( I-1 , M ) )/( I + 1 -M )
10       CONTINUE
20    CONTINUE

      RETURN
      END
```

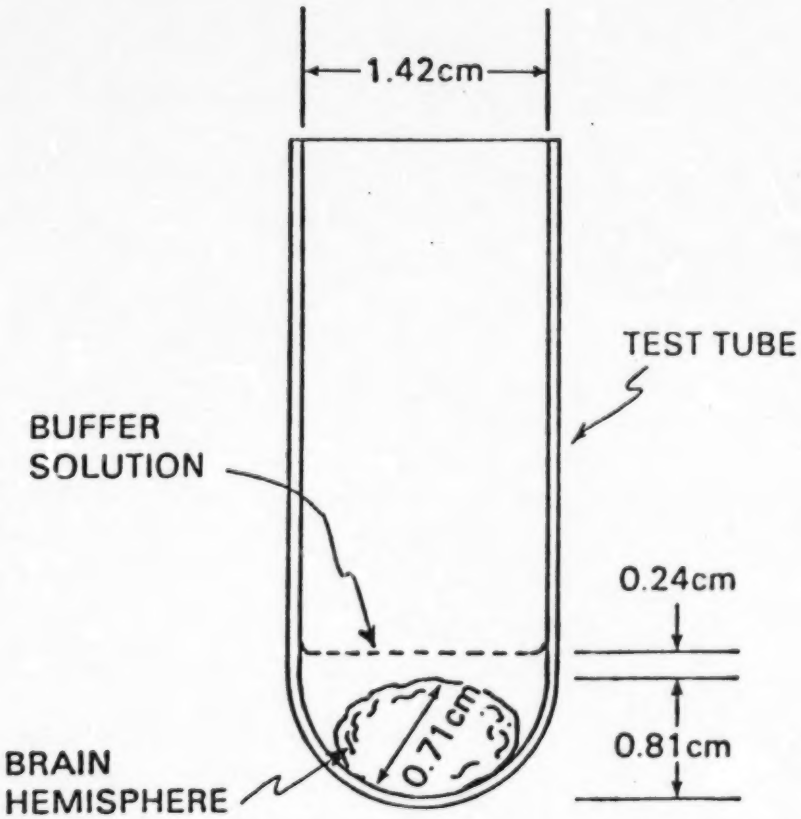

Fig. 1--Schematic of the chick ain inside a test tube containing a buffer solution.

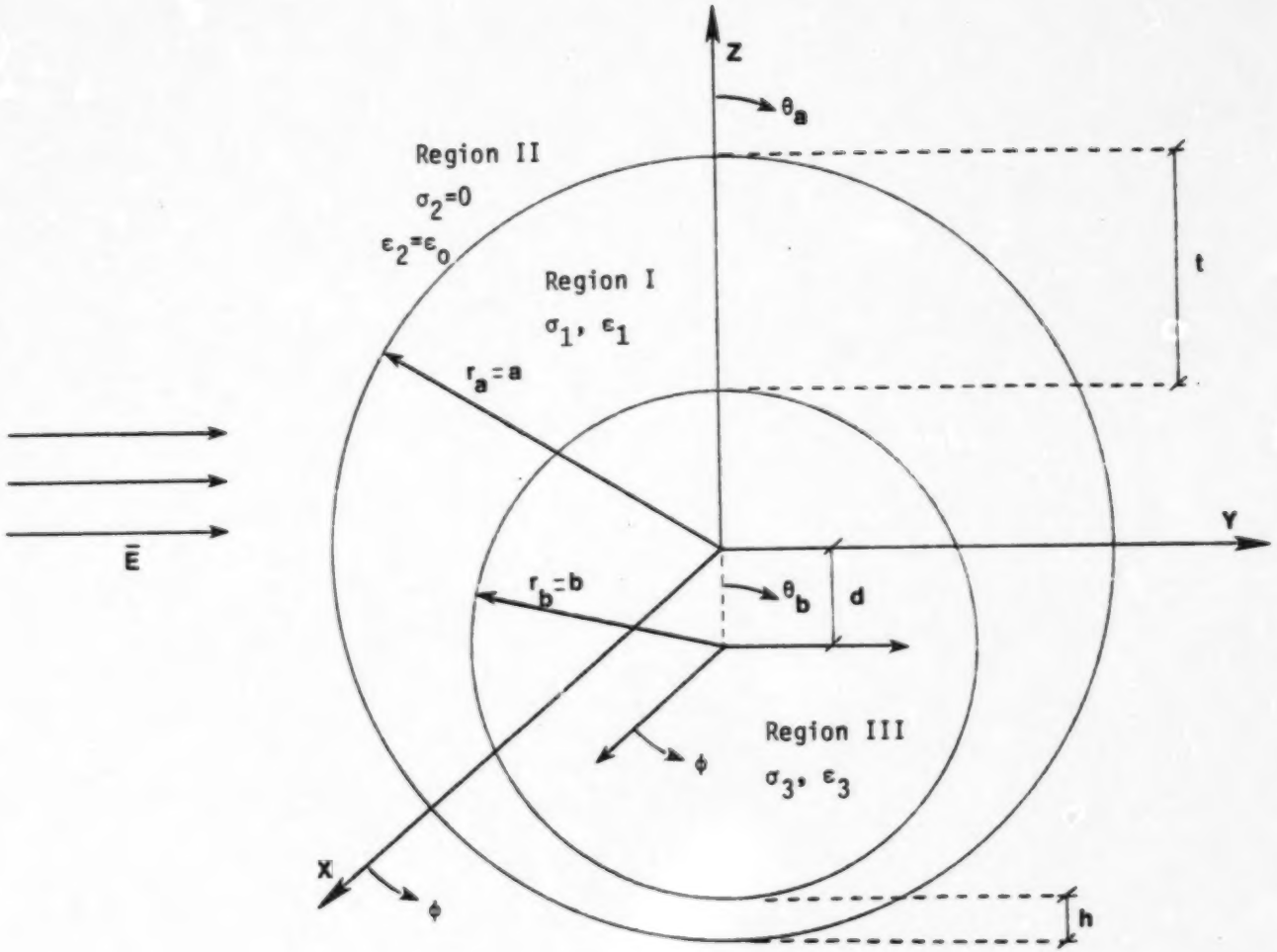

Fig. 2--Off center spherical model for the chick brain.

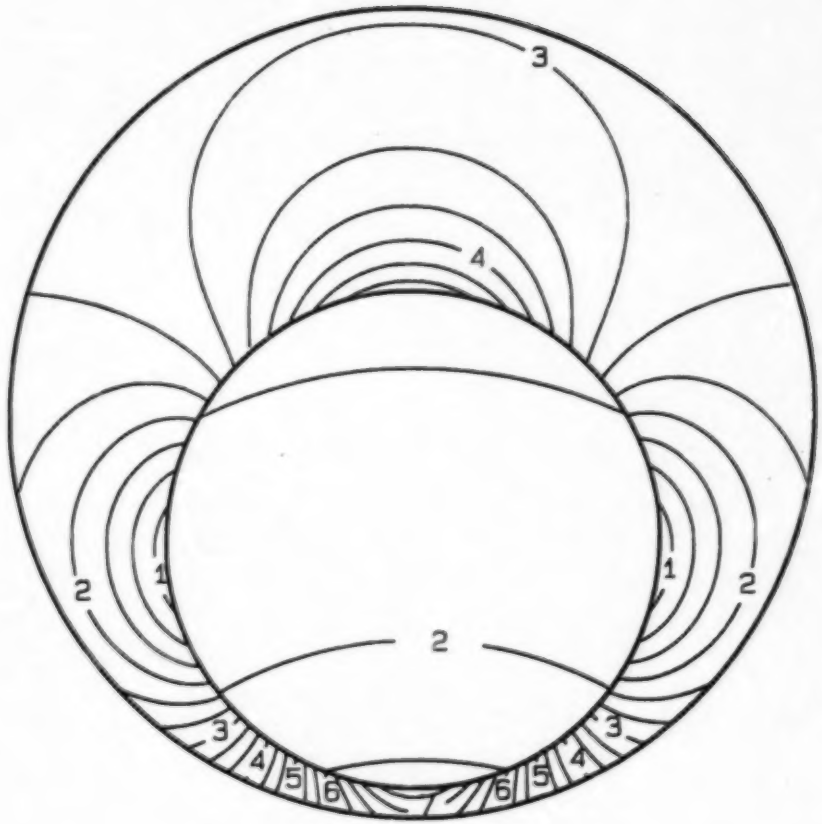

Fig. 3--Absorbed power density distribution at 50 MHz. The dimensions are a=0.677 cm, b=0.415 cm, d=0.212 cm, h=0.05 cm, and t=0.474 cm.

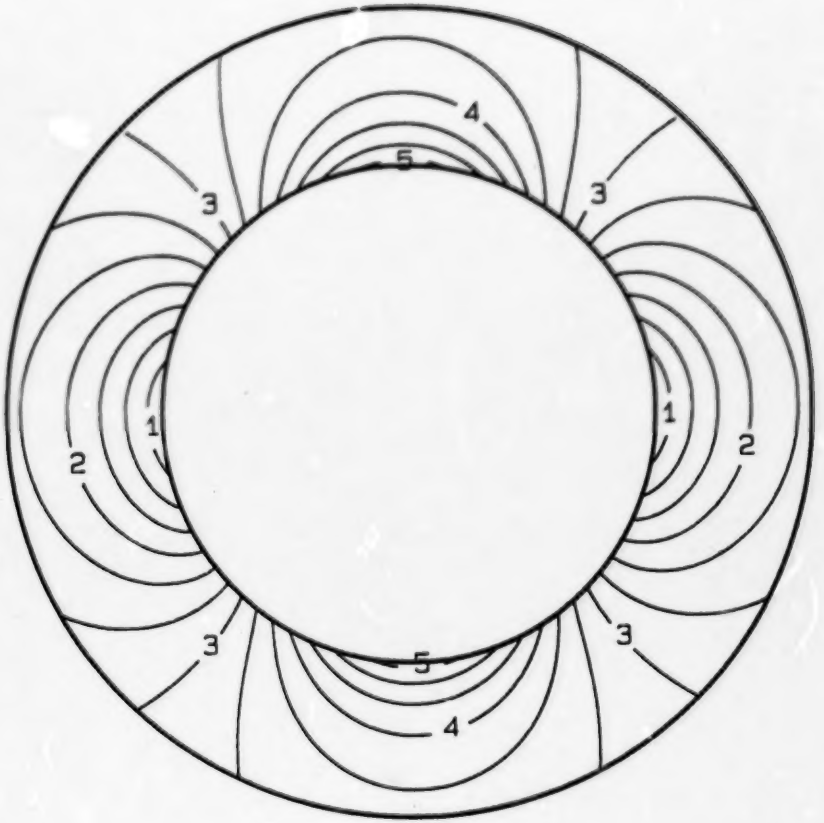

Fig. 4--Absorbed power density distribution at 50 MHz for a centered spherical model (d=0). The dimensions are a=0.677 cm, b=0.415 cm and t=0.262 cm.

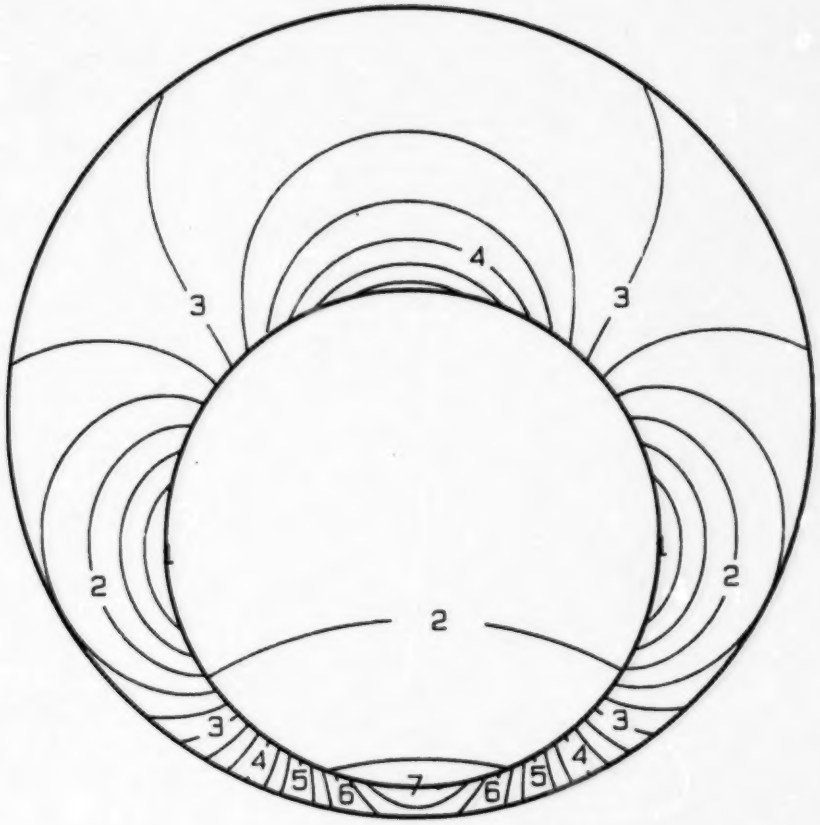

Fig. 5--Absorbed power density distribution at 100 MHz. The dimensions are a=0.677 cm, b=0.415 cm, d=0.212 cm, h=0.05 cm, and t=0.474 cm.

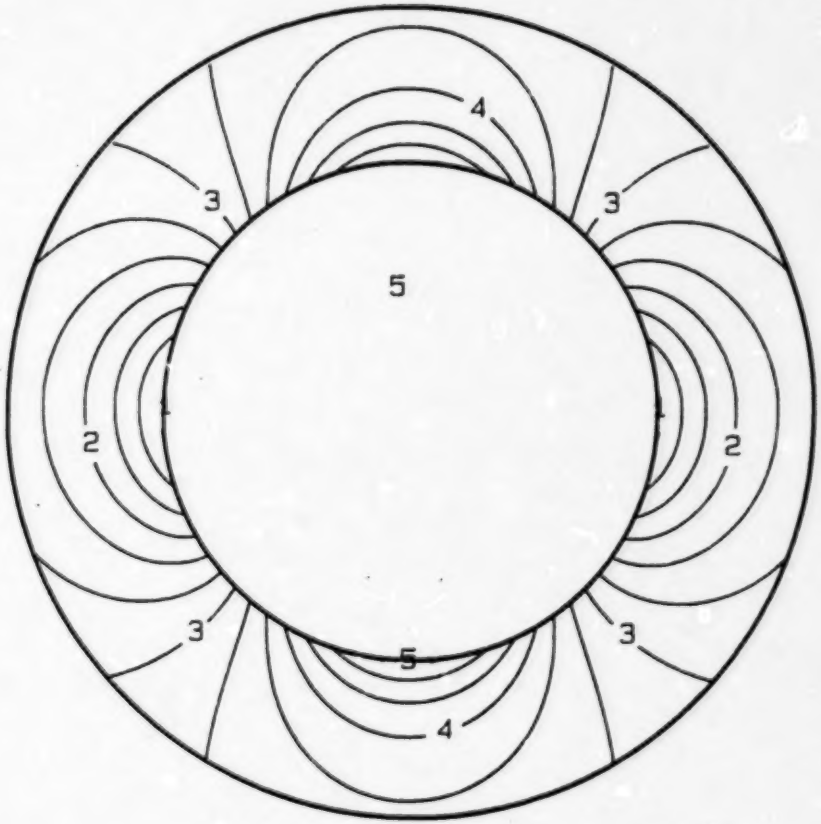

Fig. 6--Absorbed power density distribution at 100 MHz for a centered spherical model (d=0). The dimensions are a=0.677 cm, b=0.415 cm and t=0.262 cm.

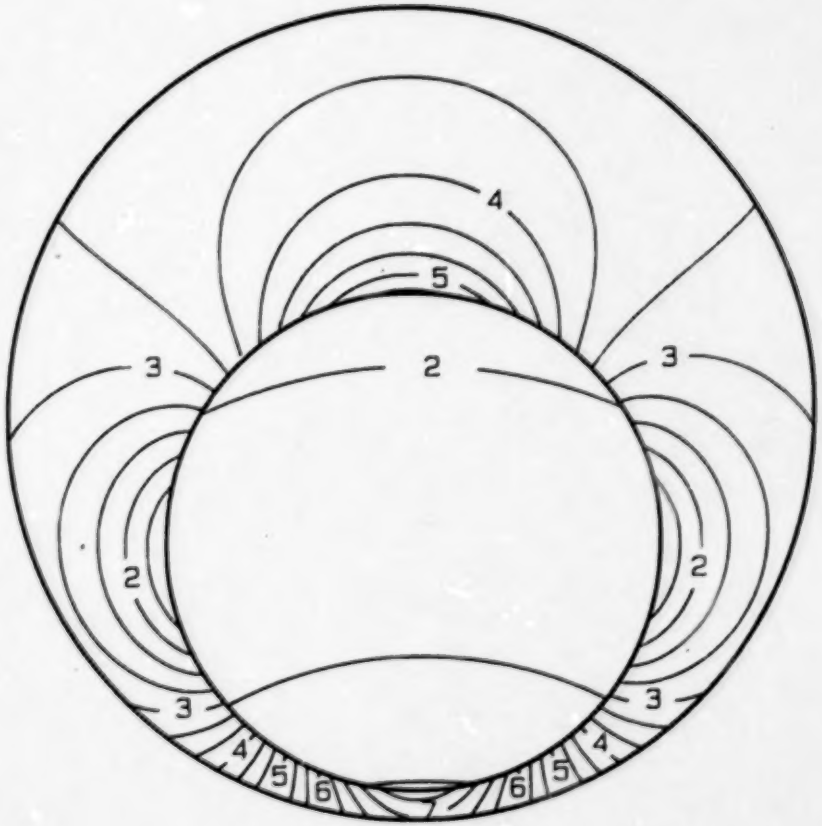

Fig. 7--Absorbed power density distribution at 147 MHz. The dimensions are a=0.677 cm, b=0.415 cm, d=0.212 cm, h=0.05 cm, and t=0.474 cm.

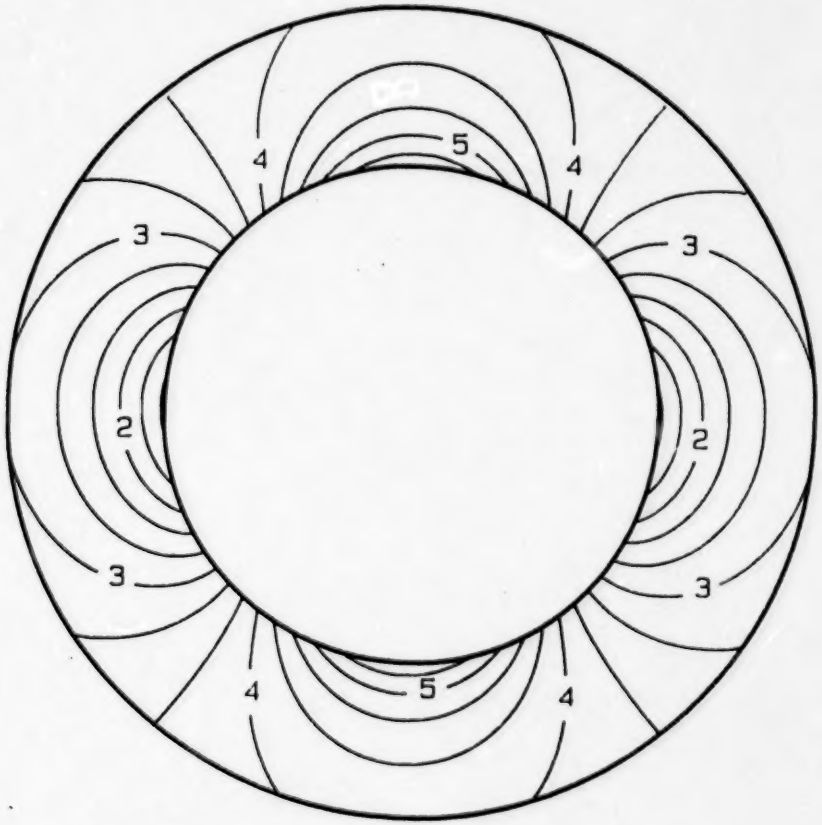

Fig. 8--Absorbed power density distribution at 147 MHz for a centered spherical model (d=0). The dimensions are a=0.677 cm, b=0.415 cm and t=0.262 cm.

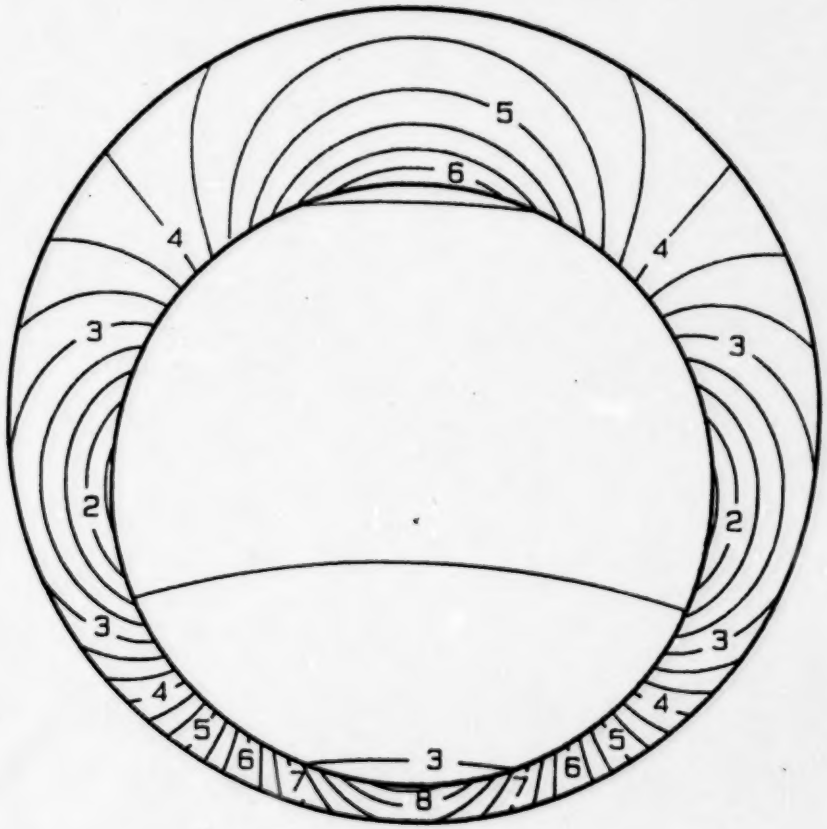

Fig. 9--Absorbed power density distribution at 147 MHz. The dimensions are a=0.56 cm, b=0.415 cm, h=0.05 cm, d=0.095 cm, and t=0.24 cm.

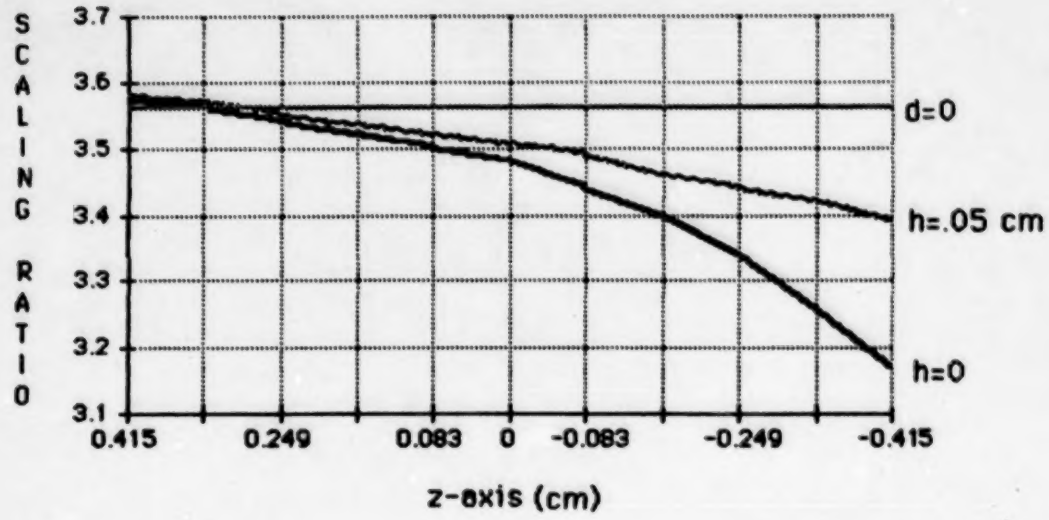

Fig. 10--Scaling ratio values for $P_i(50)/P_i(100)$ along the z-axis of the brain.

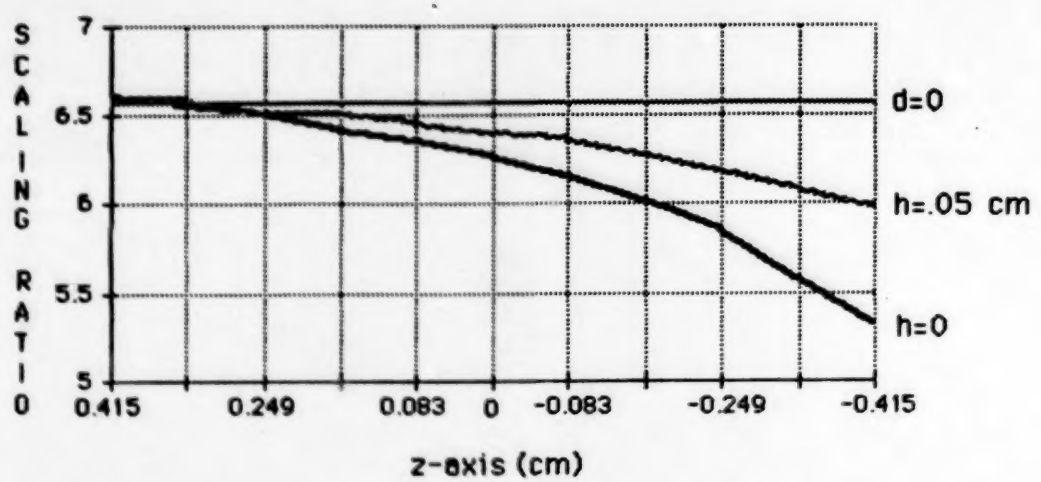

Fig. 11--Scaling ratio values for $P_i(50)/P_i(147)$ along the z-axis of the brain.

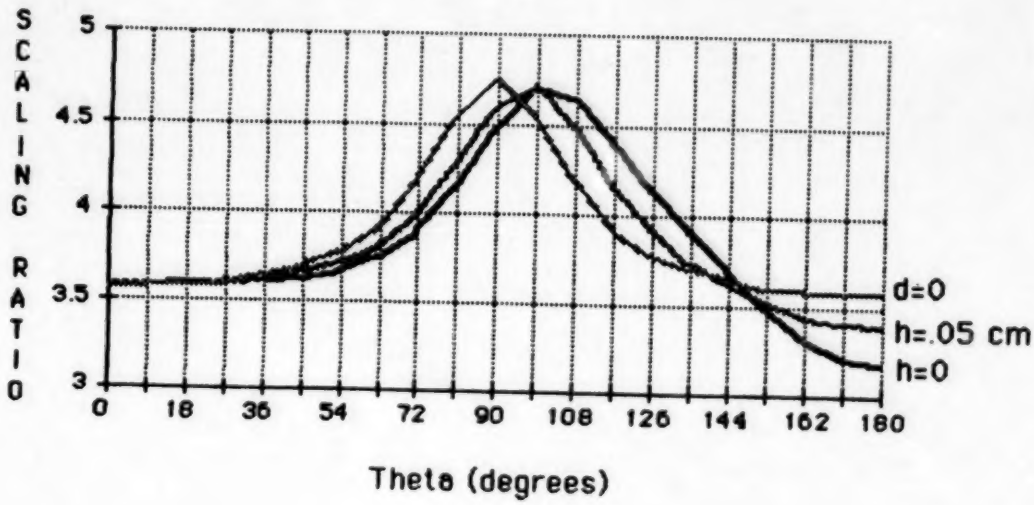

Fig. 12--Scaling ratio values for $P_i(50)/P_i(100)$ along the outside surface of the brain as a function of θ.

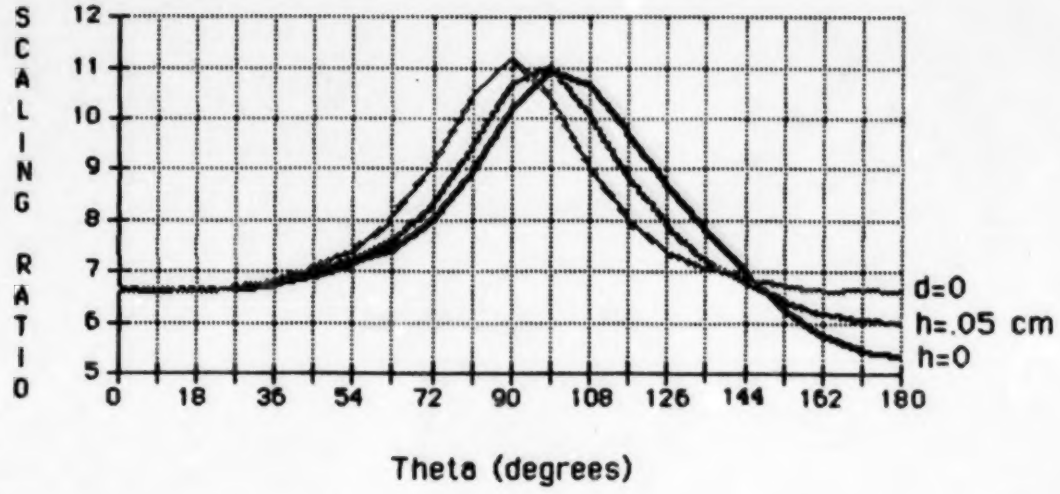

Fig. 13--Scaling ratio values for $P_i(50)/P_i(147)$ along the outside surface of the brain as a function of θ.